

Pulsed Electroluminescence in a Dopant-free Gateable Semiconductor

S. R. Harrigan,^{1,2,3} F. Sfigakis,^{1,4,5,*} L. Tian,^{1,4} N. Sherlekar,^{1,2} B. Cunard,^{1,4}
M. C. Tam,^{3,4} H.-S. Kim,^{3,4} Z. Wasilewski,^{1,2,3,4} M. E. Reimer,^{1,2,4,†} and J. Baugh^{1,2,3,5,‡}

¹*Institute for Quantum Computing, University of Waterloo, Waterloo N2L 3G1, Canada*

²*Department of Physics and Astronomy, University of Waterloo, Waterloo N2L 3G1, Canada*

³*Waterloo Institute for Nanotechnology, University of Waterloo, Waterloo N2L 3G1, Canada*

⁴*Department of Electrical and Computer Engineering,
University of Waterloo, Waterloo N2L 3G1, Canada*

⁵*Department of Chemistry, University of Waterloo, Waterloo N2L 3G1, Canada*

We report on a stable form of pulsed electroluminescence in a dopant-free direct bandgap semiconductor heterostructure that we coin the *tidal effect*. Swapping an inducing gate voltage in an ambipolar field effect transistor allows incoming and outgoing carriers of opposite charge to meet and recombine radiatively. We develop a model to explain the carrier dynamics that underpins the frequency response of the pulsed electroluminescence intensity. Higher mobilities enable larger active emission areas than previous reports, as well as stable emission over long timescales.

A pulsed form of electroluminescence (EL) has recently been discovered in ambipolar field-effect transistors (FETs) using 2D materials [1], which does not require a forward bias for light emission to occur. Instead, by periodically swapping the gate polarity of the FET, carriers already present in the FET recombine radiatively with incoming carriers of the opposite charge. Similar forms of this pulsed EL have been demonstrated in several material systems including 2D materials [1–4], bulk semiconductors [5, 6], and Si CMOS [7]. Pulsed EL is a promising candidate for light emitters with high wall-plug efficiency [8] since only a single ac signal is required for EL to be observed without the need for ac-to-dc conversion [9].

Despite these demonstrations of pulsed EL, they suffer from the following disadvantages. First, all previous implementations have a single electrical contact, which allows efficient carrier injection for only one type of carrier polarity. Carrier injection is inefficient for other carrier polarity due to the Schottky contact, thus limiting total brightness [1]. In addition, they all have low mobilities which limit EL emission to small active areas, contained within 20 μm from the single electrical contact. For 2D materials, the EL intensity decays with time (minutes/hours) through permanent device degradation [1, 3], and device fabrication methods are not yet scalable in the semiconductor industry. Finally, bulk semiconductors and Si CMOS suffer from low emission efficiency. This inefficiency is due to a lack of confinement in bulk semiconductors, and an indirect bandgap in Si CMOS.

In this Letter, we overcome the above limitations by fabricating FETs in a III-V semiconductor heterostructure without doping, well-suited for industrial scaling, efficient light emission, and large active areas. Bright EL emission is observed up to 370 μm away from the electrical contact, over an order of magnitude further away from the electrical contact than in any previous report [1–7] and limited only by the gate dimensions of our devices. Our implementation uses dedicated ohmic contacts for

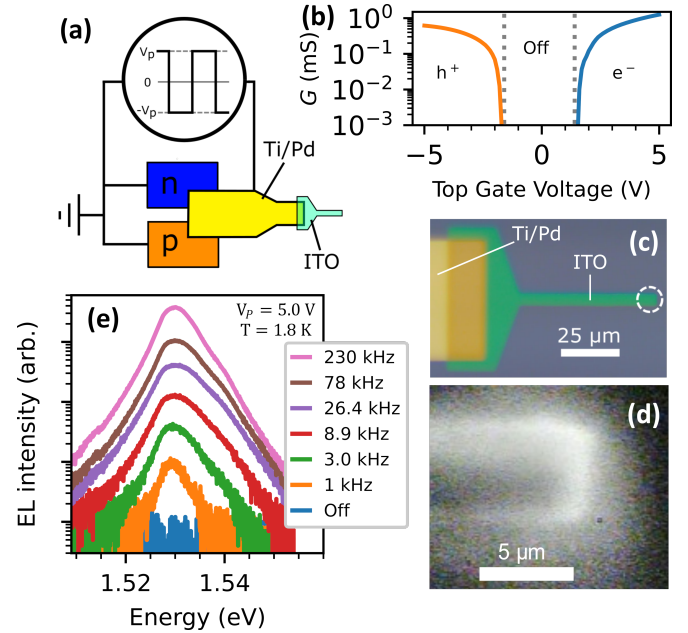


FIG. 1. (a) Schematic representation of our device and electrical circuit. N-type and p-type ohmic contacts are grounded during all measurements. An ac square wave voltage with amplitude, V_p , at swapping frequency, f_s , is applied to the top gate. (b) Typical turn-on voltages of an ambipolar FET. (c) Optical image of our device. Dashed white circle on far right is approximate collection area of the objective lens. (d) Optical image of light emission from underneath the tip of ITO gate [dashed white circle in panel (c)] for $f_s = 800$ kHz and $V_p = 5$ V. (e) Pulsed EL spectra from the tidal effect as a function of f_s .

both electrons and holes, which allows for rapid injection of both carrier types into the light emitting region. Neither EL decay nor device degradation are observed. Finally, temperature dependent measurements allows the unambiguous identification of free excitons in the quantum well driving the observed EL in the quantum well.

Dopant-free accumulation-mode GaAs-based FETs

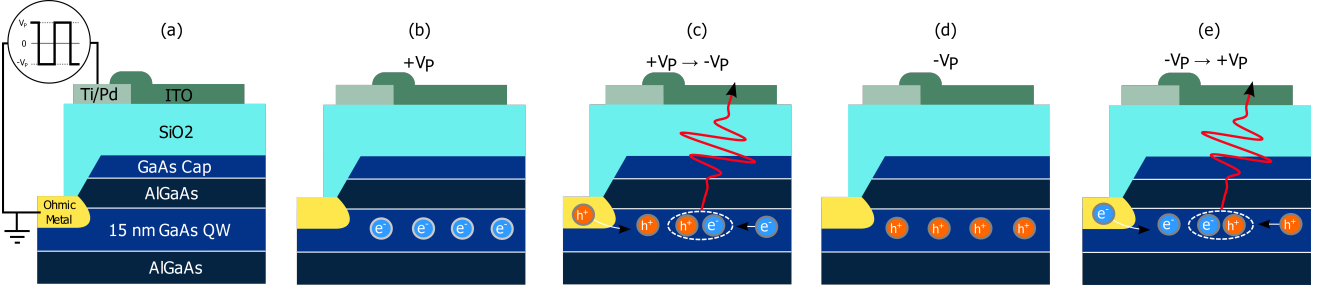


FIG. 2. (a) Schematic view of device along growth direction (not to scale) indicating relevant layers within the device. (b)–(e) Light emission mechanism of the tidal effect. (b) Initially, the gate voltage is positive, and a 2DEG is induced in the QW. (c) The gate voltage is changed from positive to negative and holes are induced from the ohmic contact and populate the QW. Simultaneous, the electrons retreat from the QW back to the ohmic contact. Some electrons and holes meet in transit and recombine radiatively, leading to a pulse of light emission. (d) After all the electrons have left the active area, a static 2DHG exists due to the negative gate voltage. (e) The gate voltage is changed from negative to positive, and a similar process to (c) occurs, except now with electrons (holes) entering (exiting) the QW.

were fabricated from a 15 nm wide quantum well (QW) heterostructure grown by molecular beam epitaxy (MBE). Both n-type and p-type ohmic contacts are present [see Fig. 1(a)], which allows the QW to be populated by either a two-dimensional electron gas (2DEG) or a two-dimensional hole gas (2DHG) in the same region underneath the gate. A 2DEG (2DHG) forms when a positive (negative) voltage beyond a threshold value is applied to the top gate [see Fig. 1(b)]. Both ohmic contacts are connected together via a common bond pad, which allows the two contacts to effectively act as one ambipolar ohmic contact [10–12]. The QW well yielded an electron (hole) mobility of $7.7 \times 10^5 \text{ cm}^2/\text{Vs}$ ($3.8 \times 10^5 \text{ cm}^2/\text{Vs}$) at a carrier density of $2.7 \times 10^{11} \text{ cm}^{-2}$ ($2.4 \times 10^{11} \text{ cm}^{-2}$) at temperature $T = 1.6 \text{ K}$ in a dedicated Hall bar [13]. Unless otherwise specified, all EL measurements were performed at $T = 1.8 \text{ K}$.

Figure 1(c) shows an optical image of the top gate at the edge of the device where EL emission is observed. Emitted light, shown in Figure 1(d), is only collected from the tip region of the transparent indium tin oxide (ITO) gate. Figure 1(e) depicts EL spectra from the same device where the intensity increases by more than two orders of magnitude as the swapping frequency, f_s , increases.

Figure 2 illustrates the mechanism for the observed EL. When swapping the polarity of the top gate voltage, the free carriers present in the QW under the gate travel towards the ohmic contact. Before reaching it, they meet the incoming carriers of the opposite charge, and recombine radiatively everywhere under the gate. We find that EL is brightest at the gate edge [Figure 1(d)]. We coin this the *tidal effect* due to the incoming and outgoing flow of carriers during every gate voltage swap. All data reported here came from one sample, but the tidal effect was observed in four samples, shown in the supplementary material [13].

Figure 3(a) plots the integrated EL intensity as a func-

tion of peak gate voltage, V_p . As expected, the brightness correlates with increasing V_p due to the higher carrier density in the QW. No EL occurs when $V_p < 1.3 \text{ V}$, in good agreement with the turn-on threshold voltage of the ohmic contacts in Fig. 1(b) [14].

We studied the EL intensity as a function of gate swapping frequency, f_s . There are two regimes depending on the interplay between $\tau_s \equiv f_s^{-1}$ and the carrier transit time, τ_{tr} , from the ohmic contact to the light collection area.

First, when $\tau_s \gg \tau_{tr}$, the EL intensity should be linearly proportional to f_s since all recombination has occurred well before the next swapping event. Figure 3(b) plots the integrated peak intensity as a function of f_s in this regime. A fit to a power law yields a best fit exponent of 0.954 ± 0.004 , in excellent agreement with this hypothesis.

Second, when τ_s is no longer much greater than τ_{tr} , not all carriers will arrive to the light collection area before the next swapping event and, as a result, the EL intensity as a function of frequency is expected to saturate and then decline with increasing f_s . Figure 3(c) shows the EL frequency response in this regime for $0.2 \leq f_s \leq 5.7 \text{ MHz}$.

To understand the observed behavior in this regime, we developed a simple model that assumes that the total EL is limited by incoming carriers arriving from the ohmic contact to the light collection area and by the dwindling outgoing carrier population from recombination. We further assume that τ_{tr} is dominated by carrier drift. The incoming carrier density at a distance x away from the ohmic contact and at time t can be approximated by a logistic-like function:

$$N(x, t) = \frac{N_0}{1 + \exp(\frac{t}{b} - \frac{x}{a})}, \quad (1)$$

where N_0 is the steady-state carrier density at a given top gate voltage, and $a, b > 0$ are fitting parameters which control the spread and average velocity of the carriers in

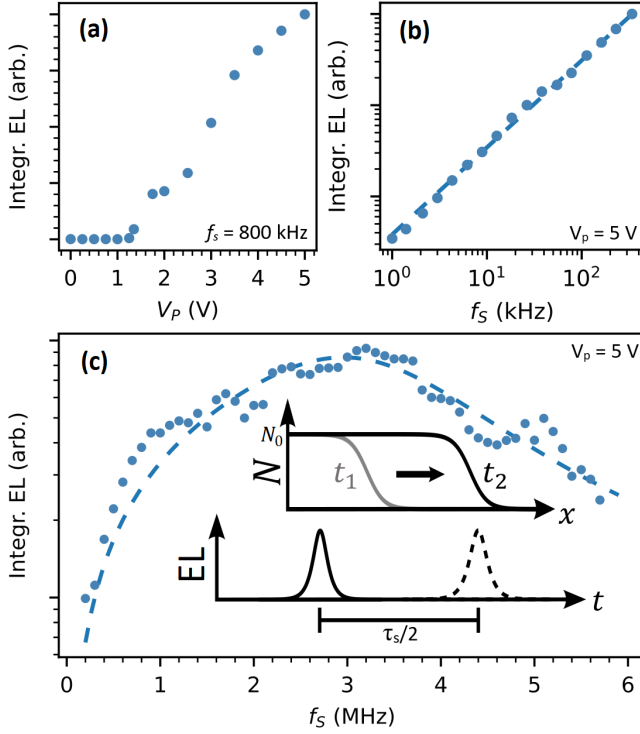


FIG. 3. (a) Integrated EL intensity as a function of peak voltage amplitude V_p . (b) Integrated EL intensity as function of swapping frequency in the low frequency regime. Dashed line is a fit to a power law. (c) Integrated EL intensity as a function of swapping frequency in the high frequency regime. Dashed line is a fit to Eq. (3) with fit parameters of $a = 64.6$ μm and $b = 44$ ns. (top inset) Schematic representation of carrier density during transit, showing propagation of incoming carriers. (bottom inset) Diagram of pulsed EL as a function of time at a fixed position. When swapping the gate at f_s , the next EL pulse will occur after time $\tau_s/2$.

transit [see inset in Fig. 3(c)]. Provided that the outgoing carriers predominantly recombine with incoming carriers, the outgoing carrier density will be given by $N_0 - N(x, t)$, since electron/hole densities are roughly the same at identical gate voltages (i.e. $N_{0,\text{electrons}} \approx N_{0,\text{holes}} \approx N_0$) [13]. Therefore, the total EL intensity will vary as:

$$I(f_s) = c f_s \int_0^{\tau_s} N(x, t) [N_0 - N(x, t)] dt, \quad (2)$$

$$= c f_s N_0^2 \left[\frac{1}{1 + \exp(-\frac{x}{a})} - \frac{1}{1 + \exp(\frac{\tau_s}{b} - \frac{x}{a})} \right], \quad (3)$$

where c is a proportionality constant.

From the fit in Figure 3(c), the effective carrier mobility can be estimated by $\mu_{\text{eff}} = \frac{v_{\text{eff}}}{E} = \frac{ad}{bV}$, where E is the electric field across the sample, v_{eff} is the average carrier velocity, d is the distance from the ohmic contacts to the light collection area, and V is the voltage difference between the ohmic contacts and the light collection area. The voltage difference across the sample is estimated to

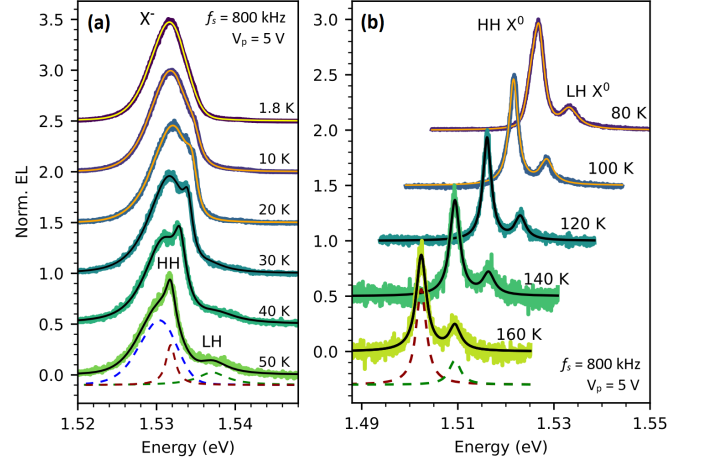


FIG. 4. Temperature dependent spectra at: (a) low temperatures and (b) high temperatures, with traces offset for clarity. Solid lines are best fits using up to 3 individual peaks (see [13] for full fit details). An example of the best fits is shown for the bottom spectra on both panels. The dashed blue curve represents an asymmetric Voigt fit [15], and the dashed green and dark red curves are fits to Lorentzians. The dashed curves are vertically offset from the data for clarity.

be E_g/e (~ 1.5 V in GaAs), as the Fermi level must go from above the conduction band to below the valence band every cycle at the ohmic contact. An effective mobility of $\mu_{\text{eff}} = 3.6 \times 10^3$ cm^2/Vs is obtained, comparable to bulk GaAs. This mobility is two orders of magnitude lower than in our reference Hall bar [13] since the first wavefront of carriers do not benefit from Thomas-Fermi screening [16, 17], the dominant mechanism for increasing mobilities in 2DEG/2DHG with increasing carrier densities.

To identify the EL emission peak in Fig. 1(e) and show that the tidal effect persists at elevated temperatures, we perform EL measurements from $T = 1.8$ K to 160 K. At $T = 1.8$ K, the EL emission spectrum is dominated by a peak centered at 1.531 eV with an asymmetric tail skewing towards lower energies [see Fig. 4(a)], consistent with the negatively charged exciton, X^- [12]. With increasing temperature, two higher energy peaks become progressively more prominent. The first is consistent with the expected emission energy (~ 1.534 eV at $T = 1.8$ K) for the heavy hole (HH) neutral exciton (X^0) in a 15 nm GaAs QW [12, 13, 18]. The second, a shallow peak at even higher energy, is attributed to the light hole (LH) X^0 [12, 19]. For $T > 80$ K [see Fig. 4(b)], X^- disappears and the two remaining peaks are attributed to HH and LH X^0 [12]. The energy splitting between the two peaks remains roughly constant from 90 K to 160 K at 6.93 ± 0.09 meV, consistent with this assignment [12]. With increasing temperature, LH X^0 becomes more prominent relative to HH X^0 , as holes transfer from the HH band to the LH band [19, 20]. In addition, the total EL intensity

decreases with increasing temperature, as routinely observed in PL experiments in GaAs QWs [21–23]. We attribute the reduction in EL due to the higher probability of carriers tunneling out of the QW as the temperature increases. We find that the tidal effect persists up to 160 K since above 160 K, no EL is observed.

In this work, we have demonstrated pulsed EL in III-V semiconductor heterostructures driven by the tidal effect for the first time. Taking into account the incoming and outgoing carriers of opposite charge, we developed a model that describes the integrated EL intensity as a function of swapping frequency, which allowed us to determine carrier transit times and mobilities. Due to faster transit times, we observed EL over longer distances from the ohmic contacts by more than an order of magnitude as compared to previous reports. We also found that the EL originated from electron-hole recombination of free excitons and trions in the QW. Furthermore, our implementation uniquely used dedicated ohmic contacts for both electron and holes, allowing for efficient carrier injection and suggests brighter EL as a result.

In the future, the area of the ITO gate can be substantially expanded, thereby increasing the total light emission area, and potentially allowing the tidal effect to be a useful mechanism to exploit for high-efficiency illumination technologies. If higher pulse frequencies (> 10 MHz) are desired, the distance between the ohmic contacts and light collection area could be reduced 100-fold while still only requiring simple optical lithography to define the gate. Our implementation utilized GaAs/AlGaAs, which emitted in the near-infrared and required cryogenic temperatures to operate. We anticipate room temperature operation in the visible spectrum by realizing ambipolar FETs in semiconductors with appropriate bandgap and barrier offsets already in use by industry. For example, green, red, and blue could be realized in GaP/AlGaP, GaAsP/InAlP, and InGaN/InAlN, respectively.

S. R. H., F. S., and L. T. contributed equally. F. S., M. E. R., and J. B. supervised the work equally. We thank members of the Quantum Photonic Devices Lab for valuable discussions. This research was undertaken thanks in part to funding from the Canada First Research Excellence Fund (Transformative Quantum Technologies), Defence Research and Development Canada (DRDC), and Canada's Natural Sciences and Engineering Research Council (NSERC). S.R.H. acknowledges further support from a NSERC Canada Graduate Scholarships-Doctoral (CGS-D). The University of Waterloo's QNFCF facility was used for this work. This infrastructure would not be possible without the significant contributions of CFREF-TQT, CFI, ISED, the Ontario Ministry of Research & Innovation and Mike & Ophelia Lazaridis. Their support is gratefully acknowledged.

* corresponding author: francois.sfigakis@uwaterloo.ca

† mreimer@uwaterloo.ca

‡ baugh@uwaterloo.ca

- [1] D.-H. Lien, M. Amani, S. B. Desai, G. H. Ahn, K. Han, J.-H. He, J. W. Ager, M. C. Wu, and A. Javey, Large-area and bright pulsed electroluminescence in monolayer semiconductors, *Nat. Commun.* **9**, 1229 (2018).
- [2] M. Paur, A. J. Molina-Mendoza, R. Bratschitsch, K. Watanabe, T. Taniguchi, and T. Mueller, Electroluminescence from multi-particle exciton complexes in transition metal dichalcogenide semiconductors, *Nat. Commun.* **10**, 1709 (2019).
- [3] Y. Zhao, V. Wang, D.-H. Lien, and A. Javey, A generic electroluminescent device for emission from infrared to ultraviolet wavelengths, *Nat Electron* **3**, 612 (2020).
- [4] Y. Zhu, B. Wang, Z. Li, J. Zhang, Y. Tang, J. F. Torres, W. Lipinski, L. Fu, and Y. Lu, A high-efficiency wavelength-tunable monolayer LED with hybrid continuous-pulsed injection, *Adv. Mater.* **33**, 2101375 (2021).
- [5] M. Hettick, H. Li, D.-H. Lien, M. Yeh, T.-Y. Yang, M. Amani, N. Gupta, D. C. Chrzan, Y.-L. Chueh, and A. Javey, Shape-controlled single-crystal growth of InP at low temperatures down to 220 °C, *Proc. Natl. Acad. Sci. U.S.A.* **117**, 902 (2020).
- [6] X. Cheng, Z. Zang, K. Yuan, T. Wang, K. Watanabe, T. Taniguchi, L. Dai, and Y. Ye, A hybrid structure light-emitting device based on a CsPbBr₃ nanoplate and two-dimensional materials, *App. Phys. Lett.* **116**, 263103 (2020).
- [7] I. K. M. R. Rahman, S. Z. Uddin, H. Kim, N. Higashitarumizu, and A. Javey, Low voltage AC electroluminescence in silicon MOS capacitors, *App. Phys. Lett.* **121**, 193502 (2022).
- [8] Wall-plug efficiency is defined as the ratio of the total optical output power to the input electrical power drawn from the power grid.
- [9] M. Zak, G. Muziol, M. Siekacz, A. Bercha, M. Hajdel, K. Nowakowski-Szkudlarek, A. Lachowski, M. Chlipala, P. Wolny, H. Turski, and C. Skierbiszewski, Bidirectional light-emitting diode as a visible light source driven by alternating current, *Nat. Commun.* **14**, 7562 (2023).
- [10] J. C. H. Chen, D. Q. Wang, O. Kloch, A. P. Micolich, K. D. Gupta, F. Sfigakis, D. A. Ritchie, D. Reuter, A. D. Wieck, and A. R. Hamilton, Fabrication and characterization of ambipolar devices on an undoped AlGaAs/GaAs heterostructure, *App. Phys. Lett.* **100**, 052101 (2012).
- [11] Y. Chung, H. Hou, S.-K. Son, T.-K. Hsiao, A. Nasir, A. Rubino, J. P. Griffiths, I. Farrer, D. A. Ritchie, and C. J. B. Ford, Quantized charge transport driven by a surface acoustic wave in induced unipolar and bipolar junctions, *Phys. Rev. B* **100**, 245401 (2019).
- [12] L. Tian, F. Sfigakis, A. Shetty, H.-S. Kim, N. Sherlekar, S. Hosseini, M. C. Tam, B. van Kasteren, B. Buonacorsi, Z. Merino, S. R. Harrigan, Z. Wasilewski, J. Baugh, and M. E. Reimer, Stable electroluminescence in ambipolar dopant-free lateral p-n junctions, *App. Phys. Lett.* **123**, 061102 (2023).
- [13] See Supplemental Material for more details on MBE growth, sample fabrication, electron/hole density and

- mobility characterization, optical measurement setup, reproducibility, EL lineshape fits, and temperature dependence of Hall bar. It includes Refs. [24–29].
- [14] In order to measure current in Fig. 1(b), both ohmic contacts must be beyond their threshold voltage. To observe the tidal effect, however, only one ohmic contact must be beyond its threshold voltage. Therefore, it is possible for the onset of tidal effect light to occur at a lower voltage amplitude than the measured electrical turn on.
 - [15] A. L. Stancik and E. B. Brauns, A simple asymmetric lineshape for fitting infrared absorption spectra, *Vibrational Spectroscopy* **47**, 66 (2008).
 - [16] T. Ando, A. B. Fowler, and F. Stern, Electronic properties of two-dimensional systems, *Rev. Mod. Phys.* **54**, 437 (1982).
 - [17] A. Shetty, F. Sfigakis, W. Y. Mak, K. Das Gupta, B. Buonacorsi, M. C. Tam, H.-S. Kim, I. Farrer, A. F. Croxall, H. E. Beere, A. R. Hamilton, M. Pepper, D. G. Austing, S. A. Studenikin, A. Sachrajda, M. E. Reimer, Z. R. Wasilewski, D. A. Ritchie, and J. Baugh, Effects of biased and unbiased illuminations on two-dimensional electron gases in dopant-free GaAs/AlGaAs, *Phys. Rev. B* **105**, 075302 (2022).
 - [18] T.-K. Hsiao, A. Rubino, Y. Chung, S.-K. Son, H. Hou, J. Pedros, A. Nasir, G. Éthier-Majcher, M. J. Stanley, R. T. Phillips, T. A. Mitchell, J. P. Griffiths, I. Farrer, D. A. Ritchie, and C. J. B. Ford, Single-photon emission from single-electron transport in a SAW-driven lateral light-emitting diode, *Nat. Commun.* **11**, 917 (2020).
 - [19] A. J. Shields, J. L. Osborne, M. Y. Simmons, M. Pepper, and D. A. Ritchie, Magneto-optical spectroscopy of positively charged excitons in GaAs quantum wells, *Phys. Rev. B* **52**, R5523 (1995).
 - [20] J. Lee, E. S. Koteles, and M. O. Vassell, Luminescence linewidths of excitons in GaAs quantum wells below 150 K, *Phys. Rev. B* **33**, 5512 (1986).
 - [21] J. S. Jiang, H. Jung, and K. Ploog, Temperature dependence of photoluminescence from GaAs single and multiple quantum-well heterostructures grown by molecular-beam epitaxy, *J. Appl. Phys.* **64**, 1371 (1988).
 - [22] A. Chiari, M. Colocci, F. Fermi, Y. Li, R. Querzoli, A. Vinattieri, and W. Zhuang, Temperature dependence of the photoluminescence in GaAs-GaAlAs multiple quantum well structure, *Phys. Status Solidi B* **147**, 421 (1988).
 - [23] G. T. Dang, H. Kanbe, and M. Taniwaki, Photoluminescence of an $\text{Al}_{0.5}\text{Ga}_{0.5}\text{As}$ /GaAs multiple quantum well in the temperature range from 5 to 400 K, *J. Appl. Phys.* **106**, 093523 (2009).
 - [24] M. P. Lilly, J. L. Reno, J. A. Simmons, I. B. Spielman, J. P. Eisenstein, L. N. Pfeiffer, K. W. West, E. H. Hwang, and S. Das Sarma, Resistivity of dilute 2D electrons in an undoped GaAs heterostructure, *Phys. Rev. Lett.* **90**, 056806 (2003).
 - [25] W. Pan, N. Masuhara, N. S. Sullivan, K. W. Baldwin, K. W. West, L. N. Pfeiffer, and D. C. Tsui, Impact of disorder on the $5/2$ fractional quantum Hall state, *Phys. Rev. Lett.* **106**, 206806 (2011).
 - [26] S. Peters, L. Tiemann, C. Reichl, and W. Wegscheider, Gating versus doping: Quality parameters of two-dimensional electron systems in undoped and doped GaAs/AlGaAs heterostructures, *Phys. Rev. B* **94**, 045304 (2016).
 - [27] R. F. Pierret, *Advanced semiconductor fundamentals*, 2nd ed., Modular series on solid state devices No. 6 (Prentice Hall, Upper Saddle River, N.J., 2003).
 - [28] R. Pässler, Basic model relations for temperature dependencies of fundamental energy gaps in semiconductors, *Phys. Status Solidi B* **200**, 155 (1997).
 - [29] S. A. Lourenço, I. F. Dias, J. L. Duarte, E. Laureto, E. A. Meneses, J. R. Leite, and I. Mazzaro, Temperature dependence of optical transitions in AlGaAs, *J. Appl. Phys.* **89**, 6159 (2001).

SUPPLEMENTARY MATERIAL

Table of Contents:

Section [I](#): MBE growth

Section [II](#): Sample fabrication

Section [III](#): Density and mobility characterization

Section [IV](#): Optical measurement setup

Section [V](#): Reproducibility

Section [VI](#): EL peak fits to temperature dependence

Section [VII](#): Temperature dependence of Hall bar

I. MBE GROWTH

The quantum well heterostructure used in this experiment, wafer G377, was grown by molecular beam epitaxy on a semi-insulating GaAs (100) substrate. Starting from the substrate, the layer order is as follows: a 200 nm GaAs buffer, a 20-period smoothing superlattice composed of a of 2.5 nm GaAs and 2.5 nm $\text{Al}_{0.3}\text{Ga}_{0.7}\text{As}$ layer, a 500 nm $\text{Al}_{0.3}\text{Ga}_{0.7}\text{As}$ barrier, a 15 nm wide GaAs quantum well, a 150 nm $\text{Al}_{0.3}\text{Ga}_{0.7}\text{As}$ barrier, and a 10 nm GaAs cap layer. No intentional dopants were placed in the heterostructure.

II. SAMPLE FABRICATION

A mesa is defined by a wet etch in 1:1:20 $\text{H}_2\text{SO}_4\text{:H}_2\text{O}_2\text{:H}_2\text{O}$ mixture. AuBe p-type and Ni/AuGe/Ni n-type recessed ohmic contacts were deposited and annealed at 520°C for 180 seconds and 450°C for 180 seconds, respectively. A 300 nm thick SiO_2 insulator layer was deposited by plasma-enhanced chemical vapor deposition. A 20/60 nm Ti/Pd top gate is deposited on top of the SiO_2 (overlapping with the ohmic contacts), and a 30 nm layer of indium tin oxide is deposited near the tip of the device.

III. DENSITY AND MOBILITY CHARACTERIZATION

A dedicated Hall bar device was fabricated in tandem with the EL samples. It was used to assess the carrier density as a function of top gate voltage and mobility as a function of carrier density at $T = 1.6$ K, as shown in Figure S1. The carrier density versus top gate voltage is linear and shows no hysteresis in the range measured (± 5 V). Electron and hole mobilities are similar to those previously reported for quantum wells in undoped GaAs with similar well width [1]. We note that significantly higher electron mobilities ($> 5 \times 10^6$ $\text{cm}^2/\text{V}\cdot\text{s}$) at similar densities has been demonstrated in undoped GaAs heterostructures by us [2] and others [3–5].

IV. OPTICAL MEASUREMENT SETUP

All optical measurements were performed in a Attocube AttoDRY 2100 optical cryostat with a base temperature of 1.6 K. Signals were generated using a Tektronix AFG1062 (rise

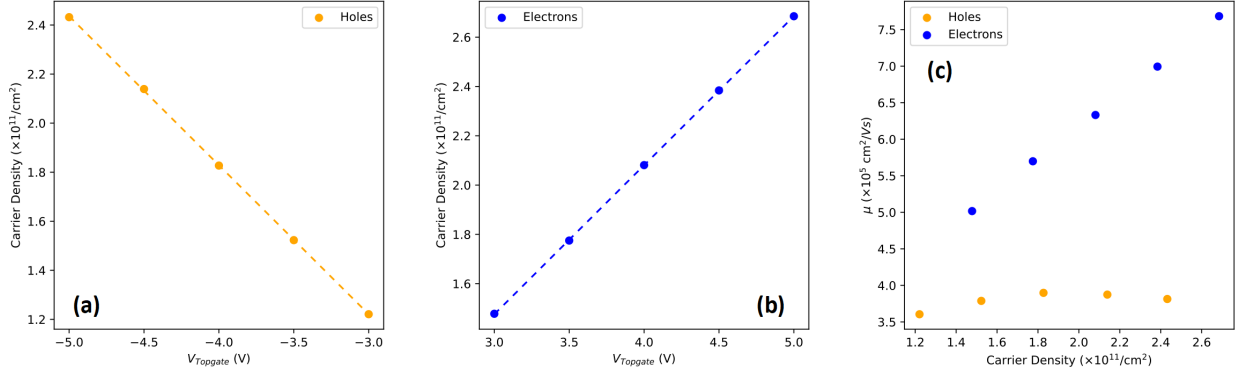


FIG. S1. (a) Hole density and (b) electron density as a function of top gate voltage. Dashed lines are linear fits. (c) Electron and hole mobility as a function of carrier density.

time $< 10 \text{ ns}$ per volt) and sent to the sample using home-built electrical feedthroughs. Light generated from the sample is collected using an Attocube LT-APO/NIR/0.81/xs objective lens and coupled in free-space to a Princeton Teledyne SP-2-750i spectrometer equipped with a PIXIS: 100BR_eXcelon CCD, using a groove density of 1200 gratings/mm.

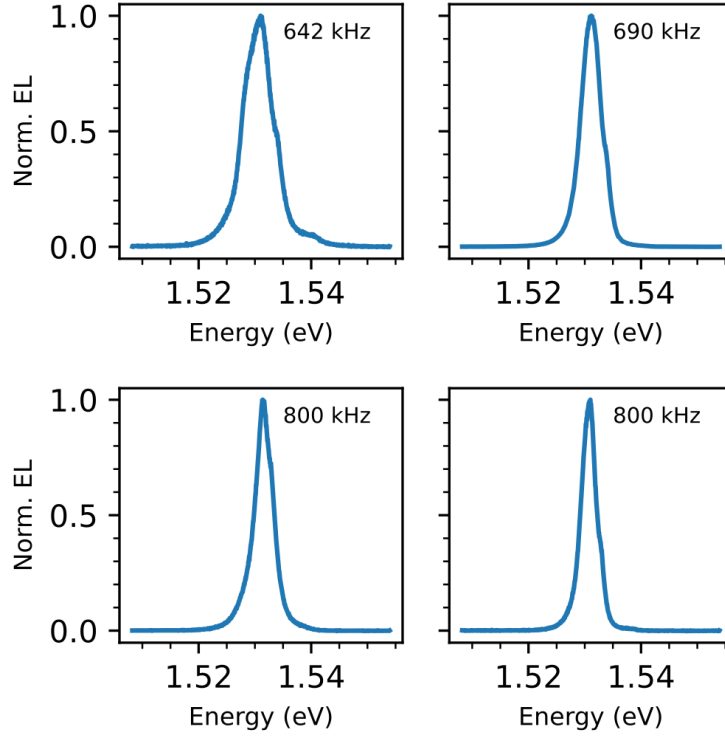


FIG. S2. EL spectrum for 4 different samples, showing reproducibility of the tidal effect. In all 4 plots, a square wave with voltage amplitude $V_p = 5 \text{ V}$ is applied to the top gate and $T = 1.8 \text{ K}$.

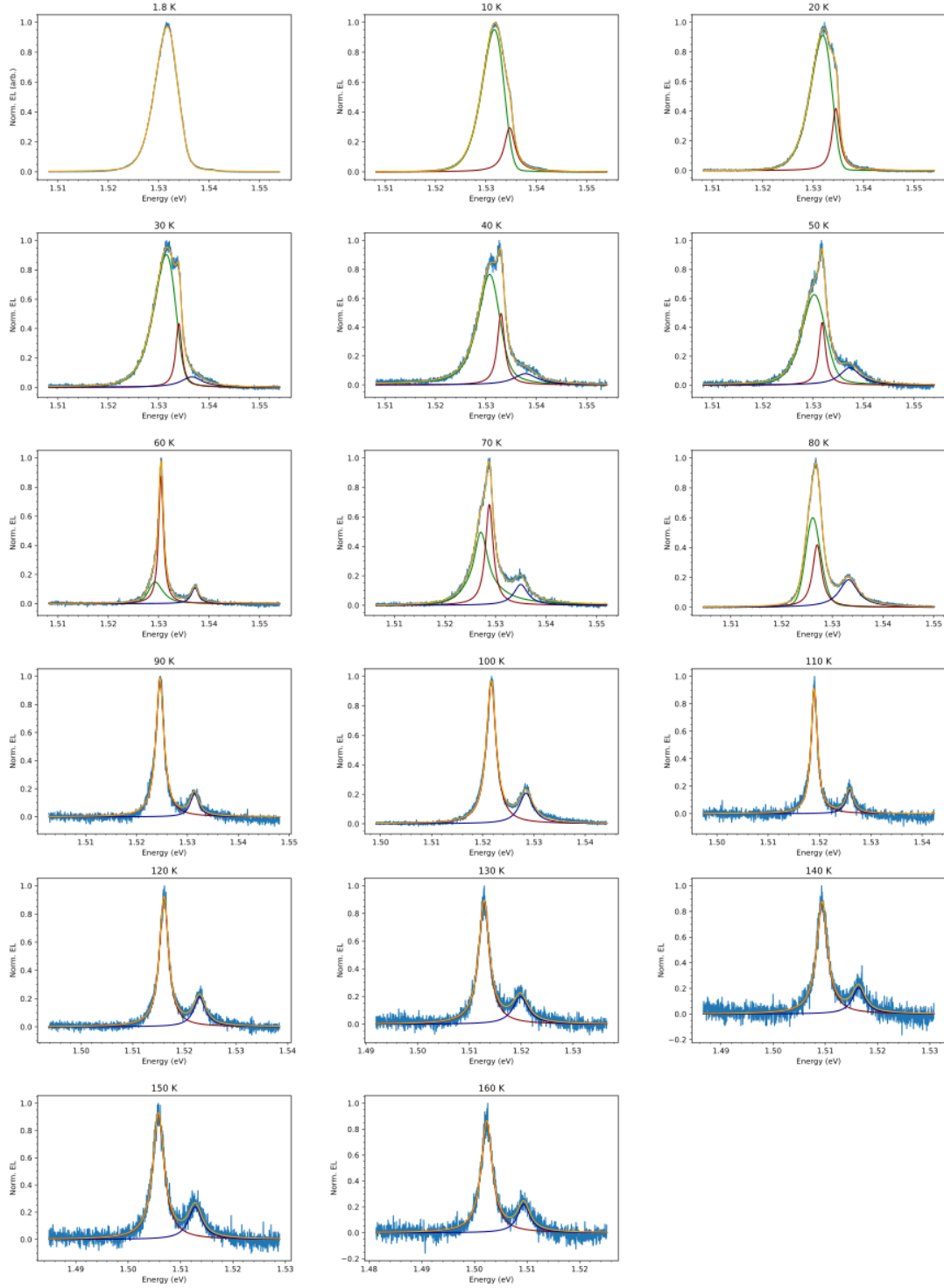


FIG. S3. Best fits of temperature dependent spectra. The light blue traces are the data and the green, dark red and dark blue traces correspond to the X^- peak, heavy hole X^0 peak and light hole X^0 peak, respectively. The X^- peak is fit to an asymmetric Voigt curve and the X^0 peaks fit to Lorentzians. The yellow curve is a sum of all curves in a given panel that yielded the best fit to the data.

V. REPRODUCIBILITY

EL spectra were acquired with 4 different samples in identical experimental conditions to show that the effect is reproducible, shown in Figure S2.

VI. EL PEAK FITS

As stated in the main text, up to 3 peaks were used to fit the spectra. The X^- peaks were fitted to an asymmetric Voigt function [6], and the light and heavy hole X^0 peaks were fitted with a standard Lorentzian. In Figure S3, we show the best fits for all the temperature dependent spectra.

Based on the fits from above, Figure S4 tracks HH X^0 as a function of temperature. From $T = 10$ K to $T = 160$ K, the emission peak red shifts by nearly 33 meV, primarily due to the decrease in the band gap energy of GaAs with increasing temperature [7]. The dashed line is a fit to the Pässler model [8] for the temperature dependence of band gap energy. The HH X^0 binding energy is found to be $E_b = 9.2 \pm 0.1$ meV, consistent with prior PL and EL measurements [1, 9].

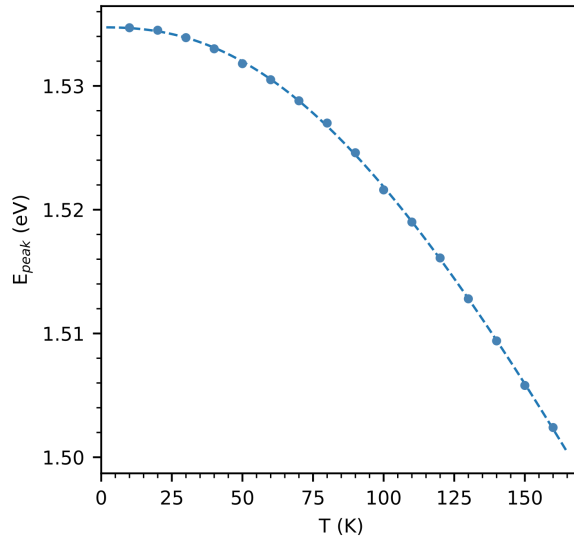


FIG. S4. EL emission energy of HH X^0 as a function of temperature, from the lineshape fits shown in Fig. S3. The dashed line is a fit to the Pässler model [8, 10].

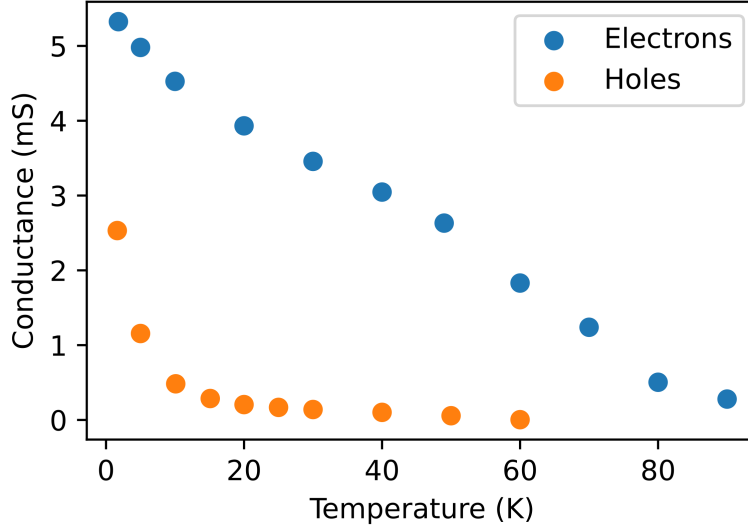


FIG. S5. Constant-voltage four-terminal conductance of reference Hall bar as a function of temperature.

VII. TEMPERATURE DEPENDENCE OF HALL BAR

Measurements on the reference Hall bar indicate the 2DEG (2DHG) loses confinement at $T = 90$ (65) K, as shown in Figure S5. The lower operating temperature of the 2DHG is consistent with smaller band offset in the valence band (~ 164 meV) compared to the conduction band (~ 217 meV) [1]. However, these temperatures do not tally with the temperature at which the tidal effect quenches (160 K). Nevertheless, from the EL emission energy (1.534 eV), the radiative recombination unambiguously occurs within the 15 nm wide GaAs quantum well, and not in the surrounding AlGaAs barriers or GaAs cap layer. At high temperature, we speculate that pulsed transient carrier populations are channelled through the quantum well, for both incoming and outgoing carriers during each swapping cycle.

-
- [1] L. Tian, F. Sfigakis, A. Shetty, H.-S. Kim, N. Sherlekar, S. Hosseini, M. C. Tam, B. van Kasteren, B. Buonacorsi, Z. Merino, S. R. Harrigan, Z. Wasilewski, J. Baugh, and M. E. Reimer, Stable electroluminescence in ambipolar dopant-free lateral p-n junctions, [App. Phys. Lett.](#) **123**, 061102 (2023).

- [2] A. Shetty, F. Sfigakis, W. Y. Mak, K. Das Gupta, B. Buonacorsi, M. C. Tam, H.-S. Kim, I. Farrer, A. F. Croxall, H. E. Beere, A. R. Hamilton, M. Pepper, D. G. Austing, S. A. Studenikin, A. Sachrajda, M. E. Reimer, Z. R. Wasilewski, D. A. Ritchie, and J. Baugh, Effects of biased and unbiased illuminations on two-dimensional electron gases in dopant-free GaAs/AlGaAs, [Phys. Rev. B **105**, 075302 \(2022\)](#).
- [3] M. P. Lilly, J. L. Reno, J. A. Simmons, I. B. Spielman, J. P. Eisenstein, L. N. Pfeiffer, K. W. West, E. H. Hwang, and S. Das Sarma, Resistivity of dilute 2D electrons in an undoped GaAs heterostructure, [Phys. Rev. Lett. **90**, 056806 \(2003\)](#).
- [4] W. Pan, N. Masuhara, N. S. Sullivan, K. W. Baldwin, K. W. West, L. N. Pfeiffer, and D. C. Tsui, Impact of disorder on the 5/2 fractional quantum Hall state, [Phys. Rev. Lett. **106**, 206806 \(2011\)](#).
- [5] S. Peters, L. Tiemann, C. Reichl, and W. Wegscheider, Gating versus doping: Quality parameters of two-dimensional electron systems in undoped and doped GaAs/AlGaAs heterostructures, [Phys. Rev. B **94**, 045304 \(2016\)](#).
- [6] A. L. Stancik and E. B. Brauns, A simple asymmetric lineshape for fitting infrared absorption spectra, [Vibrational Spectroscopy **47**, 66 \(2008\)](#).
- [7] R. F. Pierret, *Advanced semiconductor fundamentals*, 2nd ed., Modular series on solid state devices No. 6 (Prentice Hall, Upper Saddle River, N.J, 2003).
- [8] R. Pässler, Basic model relations for temperature dependencies of fundamental energy gaps in semiconductors, [Phys. Status Solidi B **200**, 155 \(1997\)](#).
- [9] A. V. Filinov, C. Riva, F. M. Peeters, Y. E. Lozovik, and M. Bonitz, Influence of well-width fluctuations on the binding energy of excitons, charged excitons, and biexcitons in GaAs-based quantum wells, [Phys. Rev. B **70**, 035323 \(2004\)](#).
- [10] S. A. Lourenço, I. F. Dias, J. L. Duarte, E. Laureto, E. A. Meneses, J. R. Leite, and I. Mazzaro, Temperature dependence of optical transitions in AlGaAs, [J. Appl. Phys. **89**, 6159 \(2001\)](#).